# Contractile Basis of Ameboid Movement VII. The Distribution of Fluorescently Labeled Actin in Living Amebas

D. LANSING TAYLOR, YU-LI WANG, and JEANNE M. HEIPLE
*Cell and Developmental Biology, Harvard University, Cambridge, Massachusetts 02138*

ABSTRACT The technique of molecular cytochemistry has been used to follow the distribution of fluorescently labeled actin in living *Chaos carolinensis* and *Amoeba proteus* during ameboid movement and various cellular processes. The distribution of 5-iodoacetamidofluorescein-labeled actin was compared with that of Lissamine rhodamine B sulfonyl chloride-labeled ovalbumin microinjected into the same cell and recorded with an image intensification microscope system. Actively motile cells demonstrated a rather uniform distribution of actin throughout most of the cytoplasm, except in the tail ectoplasm and in the plasma gel sheets, where distinct actin structures were observed. In addition, actin-containing structures were induced in the cortex during wound healing, concanavalin A capping, pinocytosis, and contractions elicited by phalloidin injections. The formation of distinct fluorescent actin structures has been correlated with contractile activities.

The distribution of individual components of the contractile cytoskeletal system must be determined in intact cells before an attempt can be made to define the molecular interactions involved in cytoplasmic structure and movement in vivo. Until recently, the distribution of actin and other proteins has been identified only in fixed cells by either electron microscopy or immunofluorescence microscopy (see reference 35 for a review). Although the techniques of electron microscopy and immunofluorescence have been valuable, only the organization and distribution of the fixed and unextracted fraction of the contractile-cytoskeletal system have been analyzed. Determining the distribution of cytoskeletal and contractile proteins has been especially difficult in the amebas *Amoeba proteus* and *Chaos carolinensis*. They move rapidly, exhibiting streaming velocities of ~1.0 μm/s, and the conversions between the gelled, solated, and contracted states occur quickly.

Electron microscopy of optimally fixed specimens of *C. carolinensis* (19, 20) demonstrated that small fibrils are readily identified parallel to the membrane in the tail cortex. In addition, Comly (7) and Taylor et al. (29) demonstrated the association of F-actin with the plasmalemma of *C. carolinensis*. The ultrastructural investigations mentioned above as well as others (i.e., Rhodes and Taylor, unpublished data) have indicated that large static actin bundles do not persist in actively motile amebas. However, all the ultrastructural information from *C. carolinensis* must be viewed with caution because the standard fixation procedures have been unable to preserve cell shape or to stabilize the cytoplasm completely (2).

The technique of in vivo molecular cytochemistry (34, see reference 37 for a review) was developed to permit the simultaneous localization and, ultimately, the characterization of specific proteins in vivo. This new technique, especially when coupled with image intensification methods and video recording (23–25, 34, 36, 39), permitted the capture and analysis of fluorescent images from living cells in real time while minimizing photobleaching damage.

We report here experiments designed to test the fate of labeled actin in living amebas and to compare its distribution with a labeled soluble protein not involved in contractile or cytoskeletal processes. The distribution and organization of cytoplasmic actin is described in this report. The question of nuclear actin (6, 12, 15) will be discussed elsewhere.

## MATERIALS AND METHODS

### *Materials*

Materials were obtained or prepared as follows. The stabilization and contraction solutions were prepared as described previously (28, 31). 0.1% Alcian blue (Pierce Chemical Co., Rockford, Ill.) was prepared in distilled $H_2O$ and brought to pH 6.5. A phalloidin (Boehringer Mannheim Biochemicals, Indianapolis, Ind.) stock solution was made to $10^{-3}$ M in 0.14 M KCl and 2.0% dimethyl sulfoxide (DMSO) (27). Concanavalin A (Con A) labeled with rhodamine (Research Plus, Bayonne, N. J.) was diluted into Marshall's culture solution (5.0



THE JOURNAL OF CELL BIOLOGY · VOLUME 86 AUGUST 1980 590-598

$\times 10^{-5}$ M $MgCl_2$, $5.0 \times 10^{-4}$ M $CaCl_2$, $1.47 \times 10^{-4}$ M $K_2PHO_4$, and $1.1 \times 10^{-4}$ M $KH_2PO_4$ at pH 7.0) (28) to a final concentration of 100 μg/ml.

## Methods

CULTURES AND CELL MANIPULATIONS: *C. carolinensis* (28) and *A. proteus* (29) were cultured as described previously and then starved for 2 d before use. Single-cell models in vitro (28) were prepared according to the published protocols. Capping of Con A in *C. carolinensis* was induced by preincubating the cells in Marshall's solution for 10 min at 4°C, treating the cells in Marshall's solution containing 100 μg/ml Con A for 5 min at 4°C, rinsing the cells with Marshall's solution at 4°C three times, and then warming the cells to room temperature (24°C). Capping occurred within 5 min. Pinocytosis was induced by rinsing the cells with the Alcian blue solution. All experiments reported were performed on at least 10 cells. Most of the observations were made on >100 individual cells over a 2-yr period.

PROTEINS AND LABELING: Actin was purified from rabbit skeletal muscle as described previously (9). The sulfhydryl specific dye, 5-iodoacetamidofluorescein (IAF) (Molecular Probes, Plano, Tex.), was used to label actin according to the published protocol (38). The details of the labeling procedure and the biochemical characterization of IAF actin are presented elsewhere (37). The purified conjugate had a dye to protein molar ratio of 0.7 to 0.9. Ovalbumin was labeled with fluorescein isothiocyanate (FITC, Sigma Chemical Co., St. Louis, Mo.) as described previously (38) or with 10% Lissamine rhodamine B sulfonyl chloride on celite (LRB, Molecular Probes, Plano, Tex.). 10 mg of LRB on celite was used to label 10 mg of ovalbumin using the same procedure described for FITC (38). The dye to protein molar ratio was estimated to be 1.6 for FITC-ovalbumin, using a molar extinction coefficient of 68,000 at 495 nm, pH 8.0, and 3.2 for LRB-ovalbumin, using a molar extinction coefficient of 13,000 at 550 nm, pH 8.0. The LRB-ovalbumin exhibited less nonspecific association with ameba cytoplasm and organelles than tetraethylrhodamine isothiocyanate (RITC)-labeled ovalbumin.

MICROINJECTIONS: The average cell volume of *C. carolinensis* is ~40 nl as determined by measuring the dimensions of monopodial cells. Approximately 1/10 of the cell volume was injected (31), and the cells exhibited no long lasting effects from microinjection. The cells were able to move, pinocytose, and phagocytose normally and remained viable for days after the injections. Micropipettes of 1.0 mm outside diameter (Frederick Haer & Co., Brunswick, Me.) were pulled on a vertical microelectrode puller (David Kopf Instruments, Tujunga, Calif.) to a final outside diameter of ~1.0 μm. The cells were injected with either FITC-ovalbumin or IAF-actin alone or a 1:1 vol:vol mixture of the LRB-ovalbumin and IAF labeled G-actin.

The labeled proteins were injected at the following concentrations: actin, 2–3 mg/ml and ovalbumin, 2–4 mg/ml. All protein solutions were dialyzed against 2.0 mM PIPES pH 6.9–7.0, 0.2 mM ATP, 0.1 mM $MgCl_2$, and 0.1 mM dithiothreitol before injection. The detectability of actin-containing structures using the image intensifier is discussed elsewhere (26 and footnote 1).

After microinjection the cells recovered quickly from the localized and reversible contractions induced by the injection process (31, 34). The labeled proteins spread throughout the cells within a few minutes, and the fluorescence intensity of actin and ovalbumin appeared relatively uniform. The rapid equilibration of the actin in the cell is consistent with a rapid turnover of endogenous filaments with the exogenous fluorescent G-actin.

The fluorescence of the labeled proteins remained uniform during at least a 12-h period in *A. proteus* and from 30 min to 1 h in *C. carolinensis*. During this period many organelles, including nuclei, were observed as objects of dark contrast in the fluorescent cytoplasm. In addition, the activity of contractile vacuoles was readily followed because they were also initially nonfluorescent. However, all labeled proteins became incorporated into vesicles within 12 h in *C. carolinensis* and ~24 h in *A. proteus*. Exocytosis was observed when fluorescent vesicles fused with the plasmalemma causing the release of fluorescent proteins into the medium.

IMAGE RECORDING: A Zeiss photomicroscope equipped with epiillumination fluorescence and Nomarski optics was used to view the cells. 16 × Plan (NA 0.32), 25 × Neofluar (NA 0.60) and 25 × oil immersion fluorescence (NA 0.80) objectives were utilized. A 60 W quartz halogen lamp was used as the light source. Zeiss fluorescein and rhodamine filter sets were used for emission and excitation. An RCA TC 1030/H image intensifier was coupled to the microscope, and the images were recorded on SONY ¾-inch video tape cassettes on an NEC video recorder. The images were viewed on an RCA television monitor.

Selected images on the video tapes were photographed on the television screen with Tri-X film, ASA 400, at ⅛-s exposures and developed in D-76 developer for 10 min at 22°C. The composite micrographs (Fig. 3) depicting Nomarski images of separate amebas were taken with Ilford HP5 film using the Zeiss automatic camera. The present study was designed to characterize the distribution of IAF-actin fluorescence. This required a comparison with LRB-ovalbumin. The rapid cell movements and the time required to change filters from fluorescein to rhodamine precluded the inclusion of Nomarski images of the same cell. Therefore, a composite figure (Fig. 3) of Nomarski images was prepared for orientation purposes.

PRACTICAL CONSIDERATIONS OF MOLECULAR CYTOCHEMISTRY: The local fluorescence intensity in cells cannot be used directly as a quantitative measure of the local concentration of labeled protein without adequate controls. The practical considerations relevant to interpreting fluorescence images from cells can be separated into two basic types: (*a*) physical and chemical and (*b*) biological. Parameters that could affect the fluorescence intensity in living cells must be considered before a complete interpretation of the fluorescence is attempted.

The fundamental physical and chemical parameters include (*a*) the local pathlength of fluorescent material, (*b*) the local chemical environment, and (*c*) the interaction of other proteins or ligands with the labeled proteins. The effect of local pathlength was controlled in the present experiments by comparing the images of IAF-actin and LRB-ovalbumin in the same cell. Controls for the local chemical environment were performed on two similar cells, one injected with IAF-actin and the other with FITC-ovalbumin. The interaction of proteins and ligands with the labeled actin is discussed elsewhere (37).

The fundamental biological quetions include: (*a*) Are the labeled actin molecules functional in the cells, and (*b*) Does the labeled actin have access to all cytoplasmic pools of actin? These questions were addressed using cell models and phalloidin injections.

## RESULTS

### The Specific Distribution of IAF-Actin in Single-Cell Models

The specific association of IAF-actin with membranes and the contractile-cytoskeletal system was demonstrated using single-cell models (28). Cells preinjected with a combination of IAF-actin and LRB-ovalbumin were incubated in the stabilization solution for 5 min and ruptured by negative pressure as described previously (28). After the rupture, the cytoplasm emptied out of the cell and separated from the plasmalemma-ectoplasm ghost (28, 29). The dynamics of this process could be followed directly, but only the final stage is presented. A large fraction of the IAF-actin fluorescence remained associated with the viscoelastic cytoplasm, whereas the LRB-ovalbumin fluorescence diffused into the surrounding medium (the volume of surrounding medium was $\sim 10^5$ times greater than the cell volume) (Fig. 1 *a* and *b*). Orienting the isolated cytoplasm with a micropipette induced the formation of birefringent (Birefringence = $10^{-4}$ (28) and fluorescent fibrils (Fig. 2 *a* and *b*). Contractions were elicited in the oriented cytoplasm by raising the free calcium ion concentration to $\sim 10^{-7}$–$10^{-6}$, which resulted in shortening of the fibrils. The fully contracted cytoplasm exhibited distinct fluorescent structures (Fig. 2 *b*) similar to the structures observed in contracted cell extracts containing labeled actin.[1] These results indicated that the IAF-G-actin rapidly equilibrated with the endogenous actin filaments.

The plasmalemma-ectoplasmic ghosts also exhibited distinct IAF-actin fluorescence, demonstrating that the labeled actin became incorporated into the endogenous membrane-associated actin pool (Fig. 1 *a*, arrow). The absence of LRB-ovalbumin fluorescence (Fig. 2 *b*) indicated that actin associated specifically with the membrane. As in all the other experiments, the results with FITC-ovalbumin were the same as those with LRB-ovalbumin. These basic experiments indicated that the labeled actin was incorporated into the endogenous pool of actin.

[1] Wang, Y. L., and D. L. Taylor. Preparation and characterization of a new molecular cytochemical probe: 5-iodoacetamidofluorescein labeled actin. *J. Histochem. Cytochem.* In press.

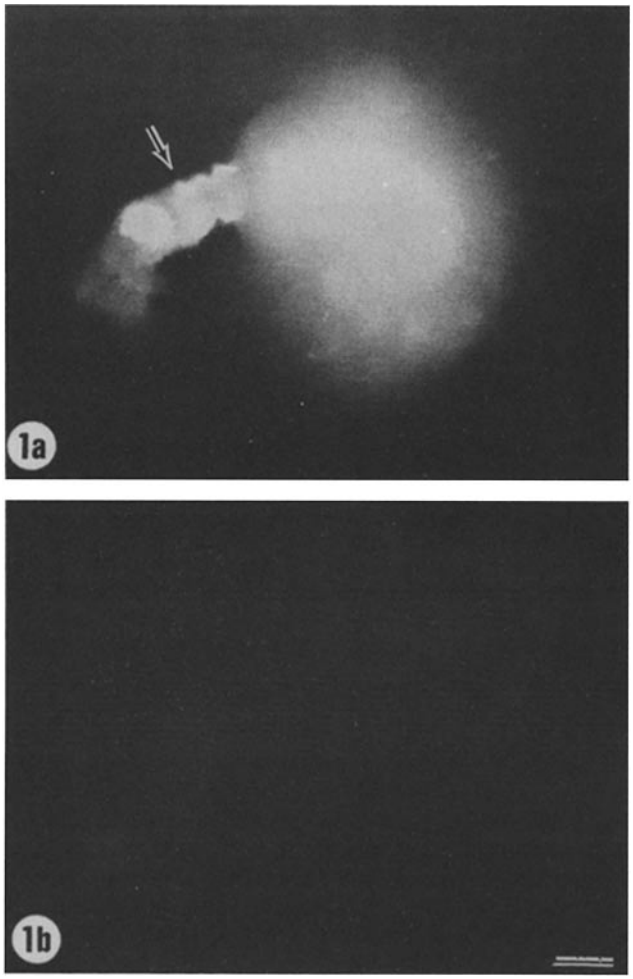


FIGURE 1 Single-cell models were prepared after injecting both IAF-actin and LRB-ovalbumin. The labeled actin remained associated with the membrane (arrow) and cytoplasm after the rupture of the cell (*a*), whereas the LRB-ovalbumin diffused away from the cell (*b*). Bar, 100 μm.

## *Cell Morphology during Ameboid Movement, Pinocytosis, Capping, and Phalloidin Injections*

Fig. 3 is a composite of Nomarski images of amebas prepared under the conditions described in this report. These images depict the average shape and morphology of an ameba tail (*a*), a tip of an extending pseudopod (*b*), a cell undergoing pinocytosis (*c*), a cell exhibiting capping of Con A receptors (*d*), a cell injected with phalloidin (*e*), and a cytoplasmic fibril (*f*). This composite is presented as a point of reference to be used when looking at the fluorescence micrographs.

## *Distribution of Actin in C. carolinensis during Normal Cell Movement*

At low magnification it was observed that the actin was distributed rather uniformly in the cell. However, actin-specific fluorescent structures similar to contracted cytoplasm (Fig. 2*b*) were sometimes observed in the tails (Fig. 4*a* and *b*).

At higher magnification, it could be seen that the most extensively wrinkled tails of motile cells (Fig. 3*a*) exhibited distinct fluorescent structures (Fig. 5*a*). Under these conditions the IAF-actin fluorescence of the tail was similar to the fluorescence observed in isolated membranes and in contracted cell models (Fig. 2*b*).[1] The distinct fluorescence remained in the tail during movement. However, the shape of the tail and the distribution of the fluorescent structures varied with time. LRB-ovalbumin controls in the same cell or FITC-ovalbumin controls in separate cells showed only diffuse fluorescence in the tail (Fig. 5*b*).

The tips of advancing pseudopods (hyalin caps) were more fluorescent than the rest of the pseudopods with IAF-actin, FITC-ovalbumin, or LRB-ovalbumin. The hyalin caps are relatively organelle free, which permits a greater accessible volume for all labeled proteins. However, when the cells were flattened to decrease the total pathlength (this decreases accessible volume), distinct fluorescent fibrils could be detected in the plasma gel sheets (Fig. 3*b*) only with IAF-actin (Fig. 6*a* and *b*). Fluorescent plasma gel sheets were much more difficult to detect in unflattened cells, probably due to the low contrast between the plasma gel sheets and the anterior cytoplasm.

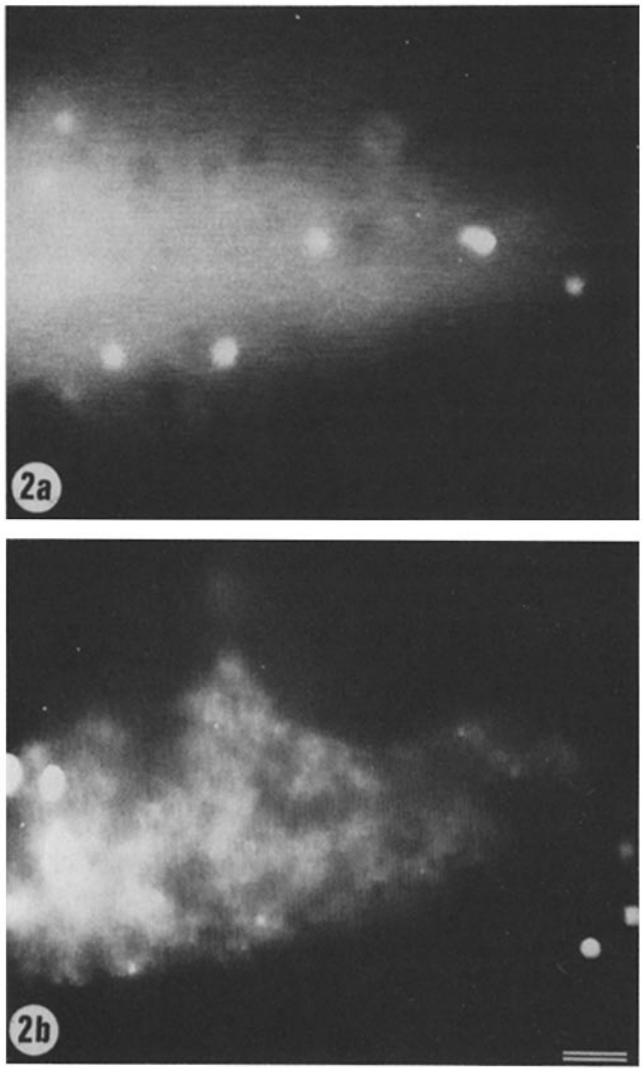


FIGURE 2 The viscoelastic cytoplasm from single-cell models containing IAF-actin could be drawn out with a micropipette, as described previously (28), and exhibited distinct IAF-actin fluorescence (*a*). Raising the free calcium ion concentration to ~$7.6 \times 10^{-7}$ M caused the fluorescent cytoplasmic fibrils (IAF-actin) to contract into fibril-containing knots (*b*). Bar, 25 μm.

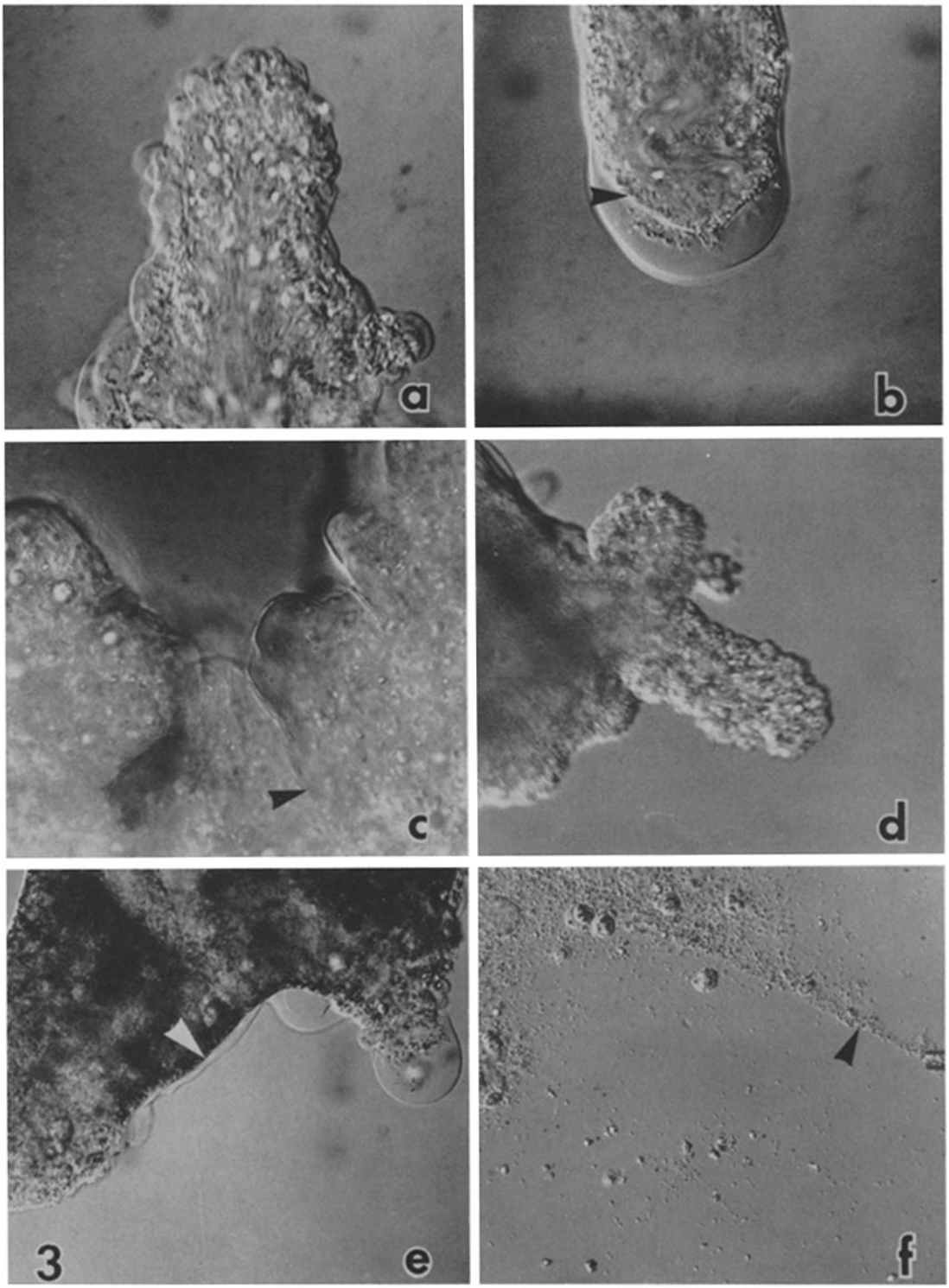


FIGURE 3 Composite images of *C. carolinensis*. Tail of an actively motile cell (*a*); the tip of an extending pseudopod (plasma gel sheet at arrow) (*b*); a small portion of the cell cortex of a pinocytosing cell (note base of pinocytotic channel, arrow) (*c*); the tail of a cell containing a Con A cap; (*e*) the formation of a cortical contracting fibril induced by phalloidin (arrow); and (*f*) a cytoplasmic fibril oriented by a micropipette (arrow).

## *Redistribution of Actin after Experimental Manipulation*

Jeon and Jeon (14) demonstrated that amebas responded to puncture wounds by forming or recruiting a large number of microfilaments at the site of damage in the cell cortex. In the present investigation, a wound-healing response was induced by micropuncture after the incorporation of labeled proteins. The refractive index of the damaged region of the cell cortex increased transiently (31), as did the IAF-actin fluorescence, which usually formed a ring that closed around the wound (Fig. 7*b*). Neither the LRB-ovalbumin control in the same cell nor the FITC-ovalbumin control in a separate cell showed any increased fluorescence at the wound (Fig. 7*a*). Within 10–15

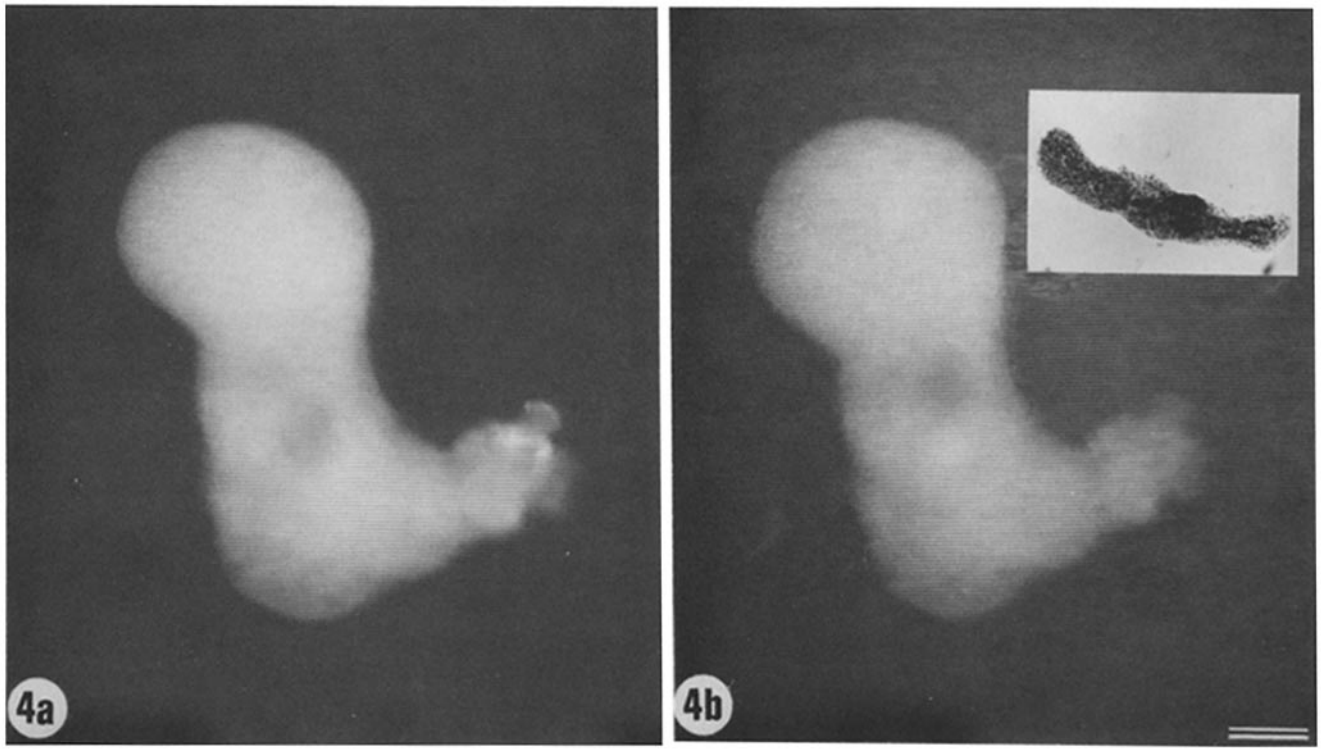


FIGURE 4 *C. carolinensis* containing IAF-actin and LRB-ovalbumin exhibited a similar distribution of actin (*a*) and ovalbumin (*b*). However, distinct fluorescent regions were readily observed in the tails of actively moving cells. Bright-field image of whole cell (*Inset* in *b*). Bar, 100 μm.

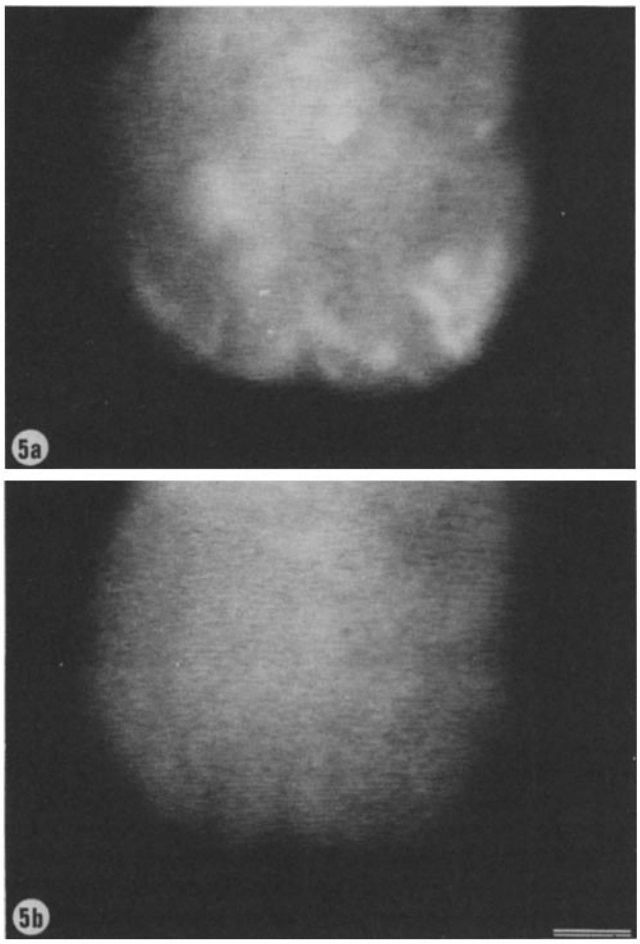


FIGURE 5 At higher magnification, tails in actively moving *C. carolinensis* exhibited many distinct actin structures in close proximity to the membrane (*a*), whereas the LRB-ovalbumin remained uniformly distributed in the same cell (*b*). Bar, 25 μm.

min, the size and fluorescence intensity of the IAF-actin fluorescent damage site decreased to the predamage conditions and the cells recovered completely. Therefore, a known change in the organization of actin was correlated with an increase in local IAF-actin fluorescence, whereas the controls exhibited no change.

A possible functional association of actin with the plasmalemma was demonstrated in our studies with *Chaos* preinjected with IAF-actin and subsequently chilled to 4°C and treated with 100 μg/ml Con A. These cells showed a dramatic redistribution of the Con A to one end of the cell when warmed from 4°C to 22°C. The capped regions became the tail (Fig. 3*d*), and the cells continued to move away from the cap. The initial Con A cap was characterized by the formation of many membrane folds (an exaggeration of a normal wrinkled tail) and a large increase in the fluorescence of the caps in cells containing IAF-actin but not FITC-ovalbumin (Fig 8*a*, *b*, and *c*). The cells sloughed off the capped surface within 20 min of formation, showing little or no internalization of the labeled Con A, and the actin returned to the more uniform distribution. This surface redistribution was similar to the basic capping phenomenon described in other ameboid cells (4, 8).

A change in the organization of actin within the cell cortex was demonstrated during the induction of pinocytosis. Treatment of cells with 0.1% Alcian blue caused the cells to stop moving (19, 20) and to form pinocytotic channels (5, 16) (Figs. 3*c* and 9, black arrow). Distinct fluorescent fibrils formed under the pinocytotic channels running parallel to the surface with IAF-actin (Fig. 9). LRB-ovalbumin actually appeared to

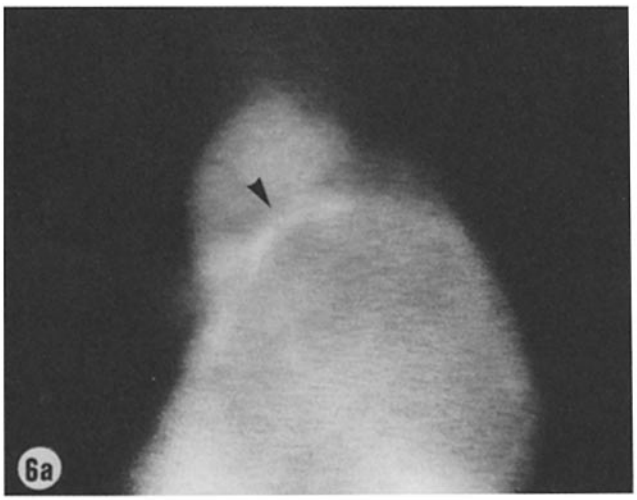


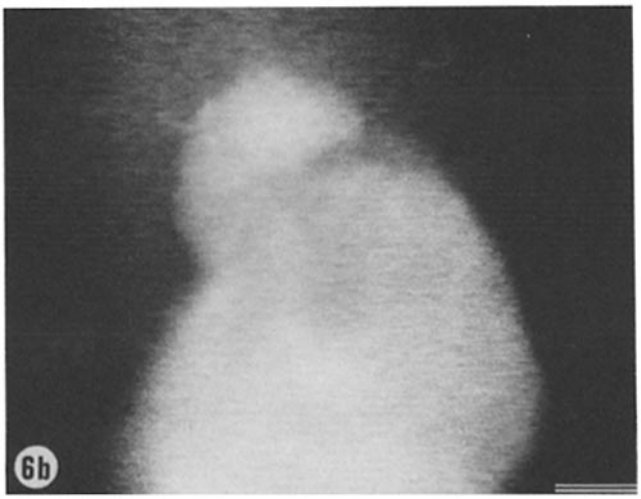


FIGURE 6 Plasma gel sheets in extending pseudopods contained actin (arrow) (*a*). The LRB-ovalbumin remained uniformly distributed (*b*). Bar, 25 μm.

be partially excluded from the cortex where actin fibrils were forming (Fig. 10).

The cyclic peptide phalloidin has been shown to cause actin polymerization, to stabilize F-actin in vitro (10), and to induce actin bundles in vivo (27). Phalloidin at a final concentration of $\sim 10^{-4}$ M was injected into *C. carolinensis* after IAF-actin and LRB-ovalbumin incorporation. Within seconds of the phalloidin injection the cells stopped moving and a distinctly fluorescent IAF-actin fibril developed in the cortex and separated from the plasmalemmas (Figs. 3 *e*, and 11 *a*). Occasionally, plasma gel sheets at the tips of advancing pseudopods were arrested and exhibited a continuity with the cortical fibrils (Fig. 11 *a*, arrow). The ovalbumin controls (Fig. 11 *b*) indicated that the structure was actin-specific. The fibrils condensed slowly to one end of the cell, forming a fluorescent intracellular knot that recruited most of the IAF-actin (Fig. 12). The final contracted state was reminiscent of the intracellular contracted fibrils and knots induced by microinjecting calcium contraction solutions (31, 34).

## DISCUSSION

### *Distribution of Actin in Living Cells*

The experiments with the single cell models (Figs. 1 and 2) and phalloidin injections (Figs. 11 and 12) were especially important in demonstrating the accessibility and functional activity of the labeled actin *in situ*. The results with the single-cell models indicated that actin was specifically and randomly associated with both the cytoplasm and the membranes (Figs. 1 and 2). In addition, induction of contraction in the fluorescent cytoplasmic fibrils demonstrated that the labeled actin participated in contraction. The results from the phalloidin injections (Figs. 11 and 12) indicated that the labeled actin was both functional and accessible to the cell cortex-membrane pool of actin. The formation of a fluorescent actin fibril arising from the cell cortex after the injection of phalloidin correlated perfectly with the ultrastructural observation reported by Stockem et al. (27), but permitted the observation of changes with time in the same cell (Figs. 11 and 12).

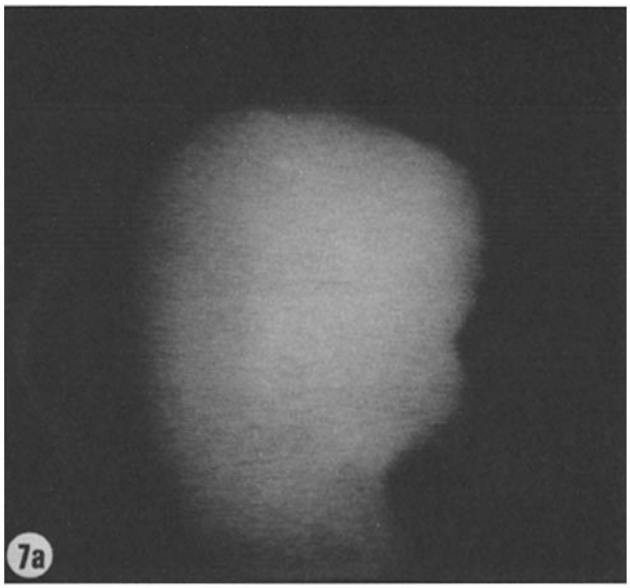


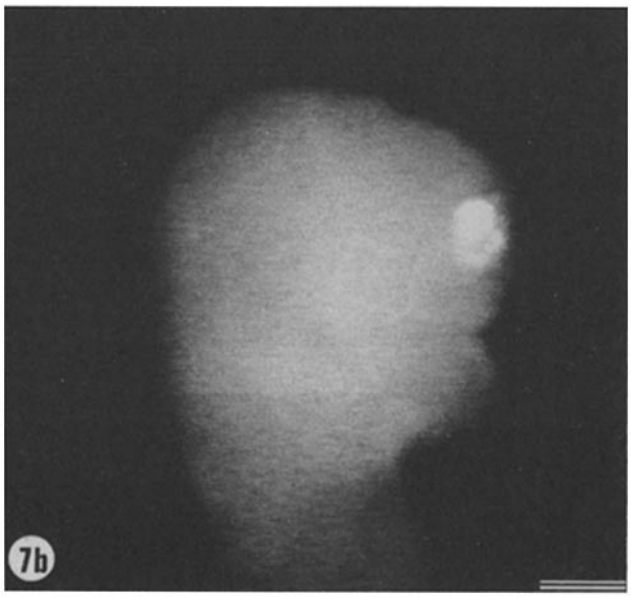


FIGURE 7 Damage response to insertion of a microneedle into the cortex of *C. carolinensis*. The IAF-actin fluorescence became distinct as the cortical wound-healing contraction was initiated (*b*), whereas no distinct LRB-ovalbumin fluorescence was observed in the wounded region (*a*). Bar, 50 μm.

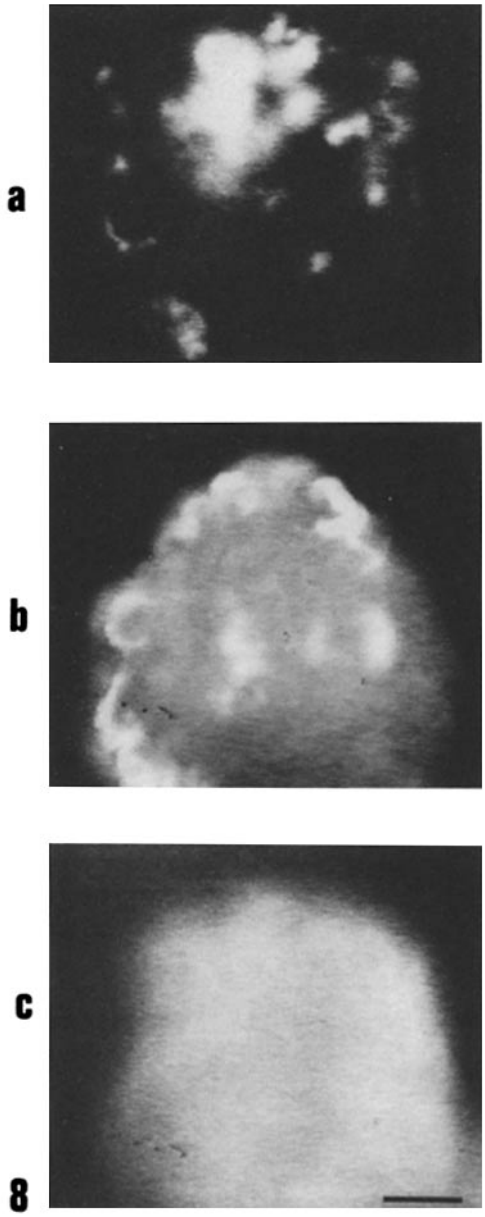


FIGURE 8 Separate cells injected with either IAF-actin or FITC-ovalbumin were treated with 100 μg/ml rhodamine-labeled Con A to induce capping. The rhodamine Con A cap formed the tail in actively moving cells (*a*). IAF-actin showed distinct fluorescence under the cap (*b*), whereas FITC-ovalbumin remained uniformly distributed (*c*). Bar, 50 μm.

Actin is distributed rather uniformly in actively moving *C. carolinensis*, and there is an absence of static actin-containing stress fibers that are present in many cells less motile than *C. carolinensis* (11, 17). However, dynamic actin structures can be detected in the tails and tips of pseudopods. The tails exhibit distinct actin structures that might be involved in generating forces for movement (18, 22, 32). This suggestion is supported by the fact that perturbations of cells that induce contractions (i.e., wound healing and phalloidin injections) always induce the formation of intensely fluorescent structures. The plasma gel sheets at the tips of advancing pseudopods contain actin structures that separate from the cytoplasmic surface of the membrane. This separation of some actin from the cortex could weaken the anterior cortical structure, thus facilitating the formation of pseudopods. The presence of other components in the plasma gel sheets will require further investigation.

The distribution of actin fluorescence in living cells can be correlated with the birefringence of living cells and some of the ultrastructure. Allen (1) demonstrated that amebas possess weak, diffuse, positive axial birefringence ($B = \sim 10^{-5}$), indicating only a small degree of submicroscopic orientation along the length of the cells. Distinct positive birefringence (parallel to the cells' along axis) was identified in the wrinkled tails and in other membrane folds on the surface of cells. In addition, distinct negative birefringence (perpendicular to the cells' long axis) was detected at the tips of advancing pseudopods. The difference in the sign of birefringence in the tails and the tips of advancing pseudopods was probably due in part to the different orientation of actin fibrils. For example, the plasma gel sheet is perpendicular to the cells' long axis so that negative birefringence would be predicted at this site. It is important to note that the highly dynamic and labile nature of the plasma gel sheets have precluded their detection by electron microscopy. Furthermore, actin fibrils have been visualized ultrastructurally, especially in the tail region (19, 20).

The formation and subsequent disappearance of actin structures during the damage response demonstrated that the cell can use the IAF-actin reversibly in cellular events. The large number of microfilaments observed by Jeon and Jeon (14) during wound healing were most likely actin and myosin filaments involved in cortical contractions. These cortical contractions can be viewed as an intracellular "clotting" mechanism because the cytoplasm is kept from emptying out of the cell. A major unanswered question is, does the actin depolymerize as part of the healing process. Future quantitative fluorescence measurements could answer this question.

The interface between the cell cortex and plasmalemma appears to be the region of active changes in the distribution and organization of actin during cellular activity. The processes of capping and pinocytosis involved distinct changes in the cortical actin distribution. The increase in actin fluorescence under the Con A caps indicated that active cortical contractions

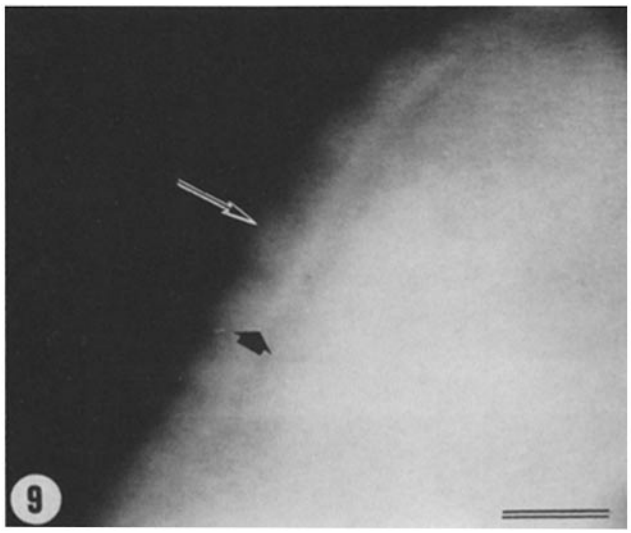


FIGURE 9 Pinocytosis induced with 0.1% Alcian blue caused the formation of an IAF-actin fibril at the base of a pinocytotic channel (short arrow). The pinocytotic channels were surrounded by blebs that gave the cell a scalloped appearance (long arrow) along the cell periphery (see reference 16 and 20 for further light and electron micrographs of pinocytotic channels). Bar, 25 μm.

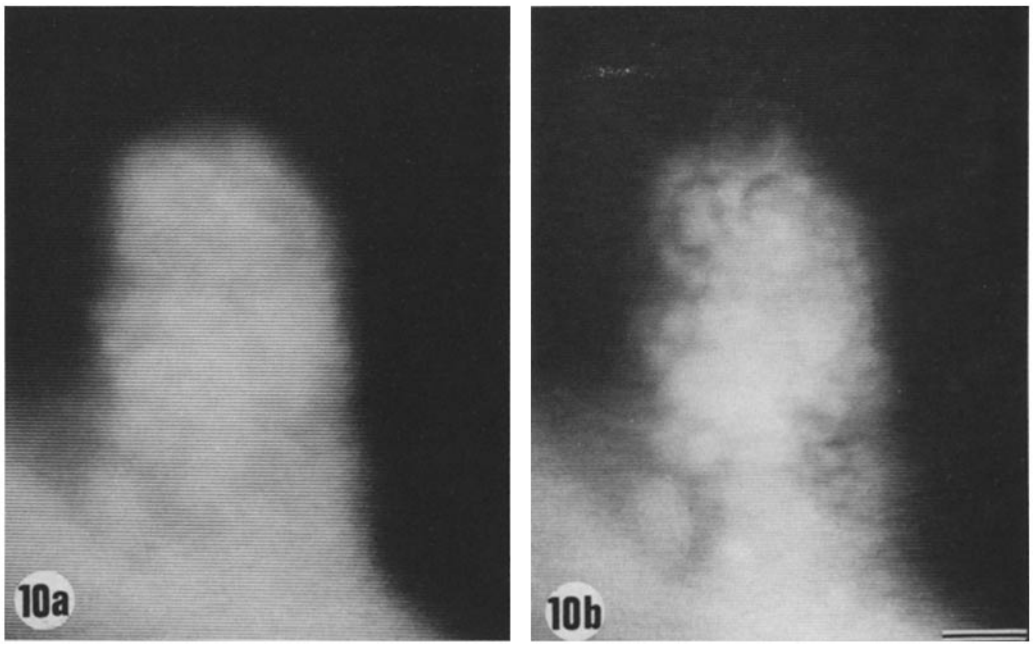


FIGURE 10 At low magnification, the pinocytotic blebs and channels exhibited IAF-actin fluorescence (*a*), whereas LRB-ovalbumin appeared to be partially excluded from the periphery of the blebs (*b*). The formation of actin bundles appeared to exclude other components. Bar, 50 μm.

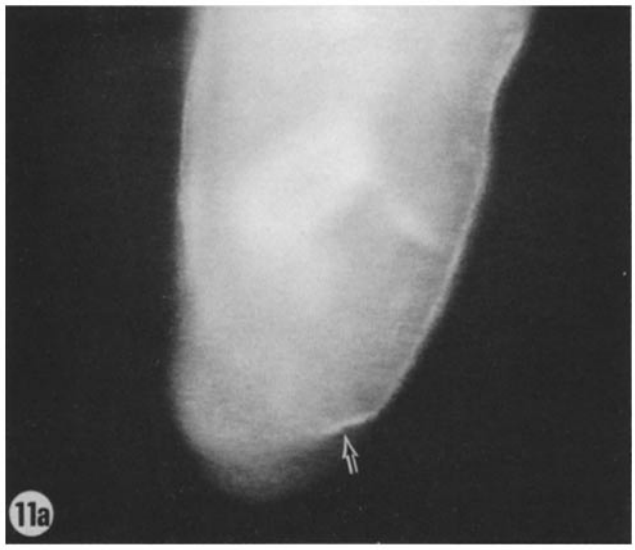


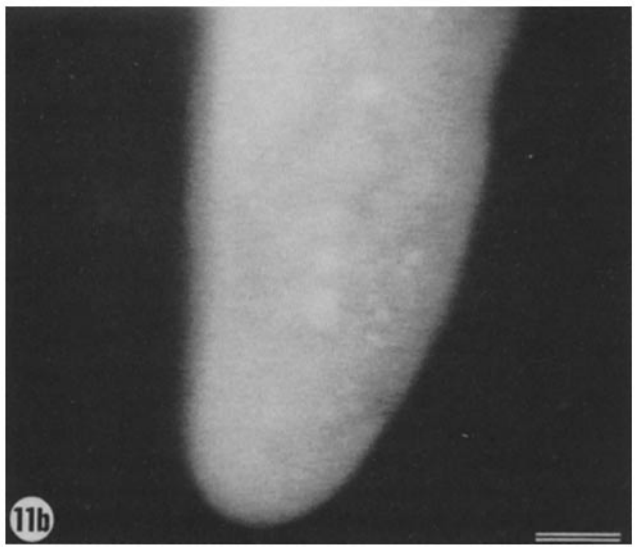


might be responsible for capping (4, 8). Furthermore, the separation of an actin fibril from the cytoplasmic side of the plasmalemma during pinocytosis suggested that uniform cortical contractions could be involved in forming pinocytotic channels. The observation that actin fibrils are present under pinocytotic channels is consistent with the concept that actin plays an active role in forming the pinocytotic channels (3, 16, 19, 20) and is probably responsible for the rounded, nonmotile state of these cells. A contracting fibrillar network forming a "cagework" on the cytoplasmic side of the plasmalemma would be expected to cause the cell to round up.

## *Functional Implication of Actin Distribution*

The giant free-living amebas move rapidly (1 μm/s) relative to other ameboid cells. In addition, the free-living cells control their shape and generate motive force apparently in the absence of cytoplasmic microtubules and 10.0-nm filaments (35). Therefore, cell shape and motility appear to be based on the actin, myosin, and gelation dynamics (see reference 35 for a review). The necessity of rapid movement involving quick changes in direction suggests the presence of a labile contractile cytoskeletal system throughout the cytoplasm. The control of structure and directed movement should then involve specific changes in the distribution of secondary messengers such as calcium and/or pH (13, 29, 30, 32). Therefore, rapid changes in secondary messengers could determine the activity and local organization of an otherwise randomly distributed system (21, 34). Actively motile ameboid cells, including fibroblasts, show a more uniform distribution of the contractile proteins (11). The formation of extensive stress fibers in fibroblasts that

FIGURE 11 The injection of phalloidin to a final concentration of $10^{-4}$ M caused the cells to stop moving and induced the formation of distinct IAF-actin fluorescence fibrils in the cell cortex (*a*). The plasma gel sheet was sometimes arrested by phalloidin and became part of the cortical fibril (arrow in *a*). The LRB-ovalbumin control in the same cell demonstrated that the fibril was actin specific (*b*). Bar, 50 μm.

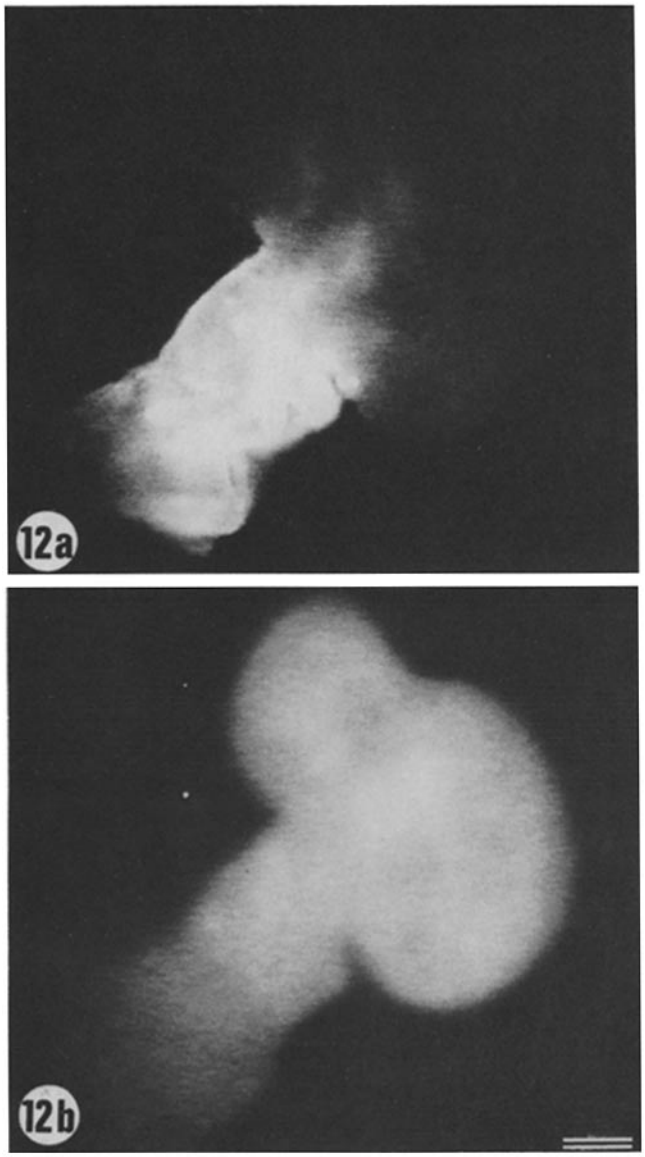


FIGURE 12 The fibril formed by injecting phalloidin contracted irreversibly to one end of the cell and recruited most of the IAF-actin into a fluorescent knot (*a*). The LRB-ovalbumin remained uniformly distributed during contraction (*b*). Bar, 100 μm.

appear as visually impressive structures actually signals a dramatic decline in motile activity. The more dispersed organization of actin and myosin (11) represents the optimal motile conditions. A correlation between the actin-based contractile events and the spatial and temporal distribution of free calcium is discussed in the following paper (36).

The authors would like to thank Dr. Elisha Haas, Dr. James La-Fountain, S. Hellewell, Dr. B. Luna, A. Strauch, V. Fowler, and S. Virgin for their helpful suggestions.

This research was supported by National Institutes of Health grant AM 18111, National Science Foundation grant PCM-7822499, and a research career development award to D. L. Taylor.

*Received for publication 6 December 1979, and in revised form 26 March 1980.*

## REFERENCES

1. Allen, R. D. 1972. Pattern of birefringence in the giant amoebae, *Chaos carolinensis*. *Expt. Cell Res.* 72:34–48.
2. Allen, R. D., and N. S. Allen. 1978. Cytoplasmic streaming in amoeboid movement. *Annu. Rev. Biophys. Bioeng.* 7:469–495.
3. Brandt, P. W. 1958. A study of the mechanism of pinocytosis. *Exp. Cell Res.* 15:300–313.
4. Braun, J., K. Fujiwara, T. D. Pollard, and E. R. Unanue. 1978. Two distinct mechanisms for redistribution of lymphocyte surface macromolecules. I. Relationship to cytoplasmic myosin. *J. Cell Biol.* 79:409–418.
5. Chapman-Andresen, C. 1977. Endocytosis in freshwater amoebas. *Physiol. Rev.* 57:371–385.
6. Clark, T. G., and R. Merriam. 1977. Diffusible and bound actin in nuclei of *Xenopus laevis* oocytes. *Cell.* 12:110–119.
7. Comly, L. 1973. Microfilaments in *C. carolinensis*: membrane association, distribution and heavy meromyosin binding in the glycerinated cell. *J. Cell Biol.* 58:230–237.
8. Condeelis, J. S. 1979. Isolation of Con A caps during various stages of formation and their association with actin and myosin. *J. Cell Biol.* 80:751–758.
9. Condeelis, J. S., and D. L. Taylor. 1977. The contractile basis of amoeboid movement. V. The control of solation, gelation and contraction in extracts from *D. discoideum*. *J. Cell Biol.* 74:901–927.
10. Dancker, P., I. Löw, W. Hasselbach, and T. Wieland. 1975. Interaction of actin with phalloidin. *Biochim. Biophys. Acta.* 400:407–414.
11. Fujiwara, K., and T. D. Pollard. 1978. Fluorescent antibody localization of myosin in the cytoplasm, cleavage furrow, and mitotic spindle of human cells. *J. Cell Biol.* 71:848–875.
12. Goldstein, L., L. Rubin, and C. Ko. 1977. The presence of actin in nuclei: a critical appraisal. *Cell.* 12:601–608.
13. Hellewell, S. B., and D. L. Taylor. 1979. The contractile basis of ameboid movement VI. The solation-contraction coupling hypothesis. *J. Cell Biol.* 83:633–648.
14. Jeon, K. W., and M. S. Jeon. 1975. Cytoplasmic filaments and cellular wound healing in *A. proteus*. *J. Cell Biol.* 67:243–249.
15. Jockusch, B., D. Brown, and H. Rusch. 1971. Synthesis and some properties of an actin-like nuclear protein in the slime mold, *Physarum polycephalum*. *J. Bacteriol.* 108:705–714.
16. Klein, H. P., and W. Stockem. 1979. Pinocytosis and locomotion of amoebae: XII dynamics and motive force generation during induced pinocytosis in *A. proteus*. *Cell Tiss. Res.* 197: 263–279.
17. Lazarides, E. 1977. Two general classes of cytoplasmic actin filaments in tissue culture cells: the role of tropomyosin. *J. Supramol. Struct.* 5:531–563.
18. Mast, S. O. 1926. Structure, movement, locomotion, and stimulation in amoeba. *J. Morphol. Physiol.* 41:347–425.
19. Nachmias, V. T. 1968. Further electron microscope studies on fibrillar organization of the ground cytoplasm of *Chaos chaos*. *J. Cell Biol.* 38:40–52.
20. Nachmias, V. T. 1964. Fibrillar structures in the cytoplasm of *Chaos chaos*. *J. Cell Biol.* 23:183–188.
21. Nuccitelli, R., M.-M. Poo, and L. F. Jaffe. 1977. Relations between ameboid movement and membrane-controlled electrical currents. *J. Gen. Physiol.* 69:743–763.
22. Pantin, C. F. A. 1923. On the physiology of amoeboid movement. *J. Mar. Biol. Assoc. U. K.* 13:1–24.
23. Reynolds, G. T. 1972. Image intensification applied to biological problems. *Q. Rev. Biophys.* 5:295–347.
24. Rose, B., and W. Lowenstein. 1975. Calcium ion distribution in cytoplasm visualized by aequorin: diffusion in cytosol restricted by energized sequestering. *Science* (*Wash. D. C.*). 190:1204–1206.
25. Sedlacek, H., H. Gundlach, and W. Ax. 1976. The use of television cameras equipped with an image intensifier in immunofluorescence microscopy. *Behring Inst. Mitt.* 59:64–70.
26. Spudich, A., and J. Spudich. 1979. Actin in Triton-treated cortical preparations of unfertilized and fertilized sea urchin eggs. *J. Cell Biol.* 82:212–226.
27. Stockem, W., K. Weber, and J. Wehland. 1978. The influence of microinjected phalloidin on locomotion, protoplasmic streaming and cytoplasmic organization in *A. proteus* and *P. polycephalum*. *Cytobiologie.* 18:114–131.
28. Taylor, D. L., J. S. Condeelis, P. L. Moore, and R. D. Allen. 1973. The contractile basis of amoeboid movement. I. The chemical control of motility in isolated cytoplasm. *J. Cell Biol.* 59:378–394.
29. Taylor, D. L., J. A. Rhodes, and S. A. Hammond. 1976. The contractile basis of amoeboid movement. II. Structure and contractility of motile extracts and plasmalemma ectoplasm ghosts. *J. Cell Biol.* 70:123–143.
30. Taylor, D. L., J. S. Condeelis, and J. A. Rhodes. 1977. The contractile basis of amoeboid movement. III. Structure and dynamics of motile extracts and membrane fragments from *D. discoideum* and *A. proteus*. *In* Cell Shape and Surface Architecture Progress in Clinical and Biological Research. Vol. 17. J. P. Reve, U. Henning, and F. Fox, editors. Alan R. Liss, Inc., New York. 581–598.
31. Taylor, D. L. 1977. The contractile basis of amoeboid movement. IV. The viscoelasticity and contractility of amoeba cytoplasm *In Vivo*. *Exp. Cell Res.* 105:413–426.
32. Taylor, D. L., S. B. Hellewell, H. W. Virgin, and J. Heiple. 1979. The solation-contraction coupling hypothesis of cell movements. *In* Cell Motility: Molecules and Organization. S. Hatano, H. Ishikawa and H. Sato, editors. University of Tokyo Press, Tokyo. 363–377.
33. Taylor, D. L., J. R. Blinks, and G. T. Reynolds. 1978. Spontaneous aequorin luminescence in *Chaos carolinensis*. *Biol. Bull.* (*Woods Hole*). 155:469.
34. Taylor, D. L., and Yu-Li Wang. 1978. Molecular cytochemistry: incorporation of fluorescently labeled actin into living cells. *Proc. Natl. Acad. Sci. U. S. A.* 75:857–861.
35. Taylor, D. L., and J. S. Condeelis. 1979. Cytoplasmic structure and contractility in amoeboid cells. *Int. Rev. Cytol.* 56:57–144.
36. Taylor, D. L., J. R. Blinks, and G. T. Reynolds. 1980. The contractile basis of amoeboid movement. VIII. Aequorin luminescence during amoeboid movement, endocytosis and capping. *J. Cell Biol.* 86:599–607.
37. Taylor, D. L., and Y.-L. Wang. 1980. Fluorescently labeled molecules can probe the structure and function of living cells. *Nature* (*Lond.*). 284:405–410.
38. Wang, Y. L., and D. L. Taylor. 1979. Distribution of fluorescently labeled actin in living sea urchin eggs during early development. *J. Cell Biol.* 82:672–679.
39. Willingham, M., and I. Pastan. 1978. The visualization of fluorescent proteins in living cells by video intensification microscopy. *Cell* 13:501–507.